J|A|C|S
COMMUNICATIONS

Published on Web 10/09/2002

Oriented Molecular Sieve Membranes by Heteroepitaxial Growth

Hae-Kwon Jeong, John Krohn, Khristina Sujaoti, and Michael Tsapatsis*

Department of Chemical Engineering, University of Massachusetts, Amherst Massachusetts 01003

Received July 10, 2002

Potential uses of crystalline molecular sieves as selective membranes, membrane reactors, chemical sensors, optical devices as well as in other new applications rely on the ability to grow them as films.[1−12] The crystallinity of these materials along with being a main advantage imposes demanding challenges for film fabrication.[3] It is well recognized that these challenges include the control of preferred orientation that is important for two main reasons. First, for most framework structures, preferred orientation can be reflected in the transport and other (e.g., optical, electronic) properties of the film.[4] Second, as it was shown recently for the case of MFI, different orientations can result in differences of the grain boundary structure which in turn influences the overall performance of a film, especially in membrane applications.[12] Other effects have been reported, as for example, on the surface roughness and optical transparency.[10] Many studies have attempted to provide methods for achieving preferred orientation in molecular sieve films. Jansen et al.[13] first discovered in situ preparation conditions that lead to *b*-out-of-plane oriented and intergrown MFI layers on silicon wafers, and this approach was recently extended by Yan and co-workers,[7] demonstrating that control of nucleation and growth can provide the means of achieving preferred orientation. However, because of insufficient understanding of nucleation and growth processes in hydrothermal systems, especially with respect to controlling particle-shape evolution and nucleation density on arbitrary supports, the success of in situ methods in yielding oriented films is limited to few zeolites and orientations. Alternative approaches to in situ growth that attempt to decouple nucleation from growth rely on pre-seeding the support of the molecular sieve film with a seed layer of particles or fragments of the same material.[8−12,14−16] Seed deposition techniques include deposition from colloidal suspensions by physical[9−12] or chemical means[8] or both with[15,16] or without[12,14] modification of the molecular sieve or support surface, rubbing,[17] laser ablation,[14] and in some cases, in situ growth.[18] Seed layers can be preferentially or randomly oriented. In the first case, epitaxial growth can lead to oriented films,[8,9,15] while in the case of randomly oriented layers preferential orientation can gradually develop as the film thickens by evolutionary selection (Van der Drifts growth).[10] Secondary growth of seed layers has been reported to result in preferentially oriented films. However, the success is still limited by available shapes/sizes and deposition methods of seed particles and by constraints in adjusting the relative crystal plane growth velocities.

In an effort to extend the secondary growth method to other molecular sieve types and orientations, we report here the formation of a preferentially oriented film of one molecular sieve (ETS-10) filling the space between preoriented needles of another (ETS-4) by heteroepitaxial growth.

ETS-10 is a microporous material consisting of [TiO_6] octahedra and [SiO_4] tetrahedra[19] while a structurally related material, ETS-4, has [TiO_5] pyramidal-squares as well as octahedral titania and tetrahedral silica.[20] ETS-10 has a tetragonal structure with the ideal composition of $M_2TiSi_5O_{13}{\cdot}nH_2O$ (M = K, Na).[19] In ETS-10, there are 12-membered rings (12MR) in all three directions, with straight channels in the *a*- and *b*-directions and nonlinear channels along the *c*-direction. The disordered structure of ETS-10 was proposed by Anderson et al.[19] as an intergrowth of two hypothetical ordered polytypes, one of which (polytype A) has chiral pore structure possessing a spiral channel along the *c*-direction. ETS-4 is also faulted and can be described as an intergrowth of four hypothetical ordered polytypes, with the ideal composition of $M_8Ti_5Si_{12}O_{38}{\cdot}nH_2O$ (M = K, Na).[20,21] In ETS-4, 12 MRs are blocked by the pronounced stacking disorder along the *c*-direction, and as a result, transport is controlled by a 2-D channel system with limiting 8MR openings. ETS materials have potential applications in catalysis, adsorption, and ion exchange as well as in membrane separations.[18,22] In addition, they have interesting optical properties due to the monatomic quantum wire character of the corner-sharing titania chains.[23]

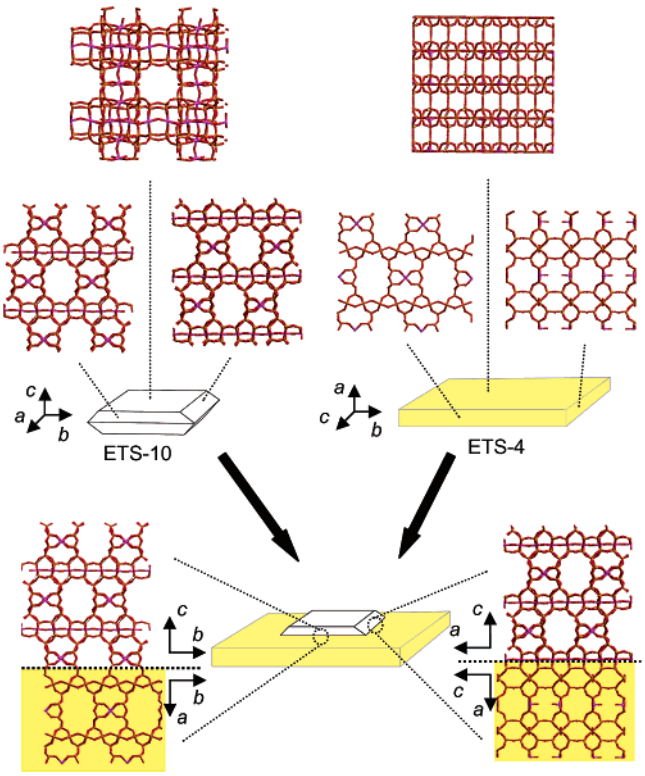

Figure 1. Structure model of heteroepitaxial growth of ETS-10 on ETS-4. (Purple: titanium. Yellow: silicon. Red: oxygen.

We have identified conditions where ETS-10 crystals are grown epitaxially on (*h*00) faces of ETS-4. Epitaxial growth of cancrinite (CAN) on certain faces of sodalite (SOD) single crystals prepared

* Corresponding author. E-mail: tsapatsi@ecs.umass.edu.

10.1021/ja020947w CCC: $22.00

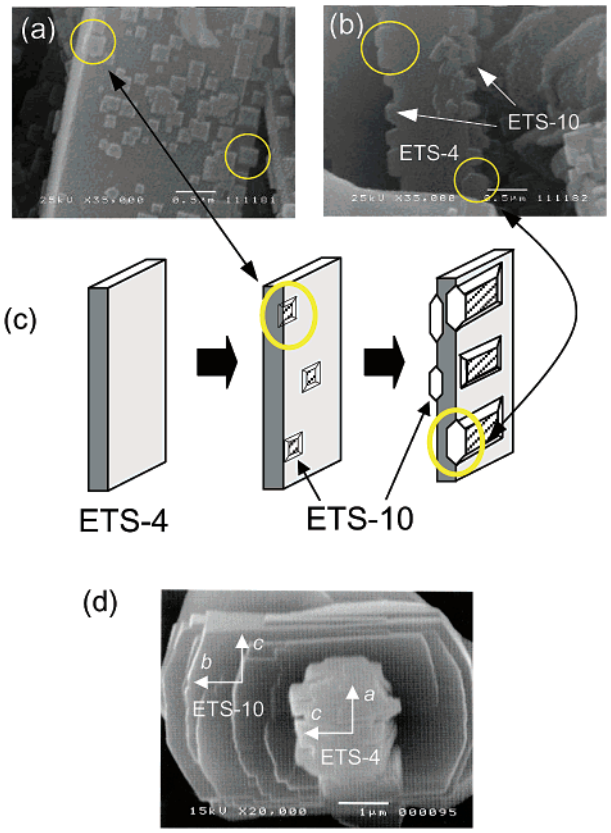

Figure 2. SEM images of heteroepitaxially grown ETS-10 crystals on ETS-4. (a) View of the (*h*00) face of ETS-4 with nucleated submicron crystals of ETS-10; (b) view of the (00*l*) face of the ETS-4 crystals; few of the ETS-10 crystals extend over the (*h*00) face and start covering the (00*l*) faces of ETS-4. A schematic of the early growth process is shown in (c). (d) Late stage of growth where the ETS-4 crystal is surrounded by ETS-10. ETS-4 and ETS-10 crystallographic directions are indicated.

by mechanical polishing was reported by Okubo et al.,[24] and several other similar zeolite cases are established in the literature.[25−27] However, this is the first report for titanosilicate molecular sieves. A structural model of the ETS-4/-10 interface is illustrated in Figure 1. The *b*- and *c*-axes of ETS-4 are parallel to the *a* (or *b*)-axis of ETS-10 with the ETS-10 *c*-axis perpendicular to the (*h*00) planes of ETS-4. There is a reasonable match of unit cell dimensions on the interfacial planes of ETS-4 ($b = 7.23$ Å, $c = 6.97$ Å) and ETS-10 (a, $b = 7.48$ Å), considering the established flexibility of these frameworks.[22] Moreover, we can identify more than one way to fully connect the (*h*00) planes of ETS-4 with the (00*l*) planes of ETS-10 in an epitaxial relationship. Figure 1 illustrates one of these. By extensive model building, we could not identify a similar match in terms of dimensions and connectivity between the other expressed faces of ETS-10 and ETS-4.

Figure 2 shows representative experimental data that corroborate the model described above. It shows SEM images of the epitaxially grown ETS-10 crystals on ETS-4. One can observe the ETS-10 crystal growth on the ETS-4 substrate with in-plane as well as out-of-plane orientation in Figure 2a. Figure 2a,b indicates that the ETS-10 crystals start growing on the (*h*00) planes of the ETS-4 and not on any of the other faces. When ETS-10 crystals eventually extend over the edge of the (*h*00) faces, they start covering the (00*l*) faces of ETS-4 indicated by the circles in Figure 2a,b. More results using ETS-4 powder and large single crystals are available as Supporting Information.

We used this epitaxial growth in the formation of oriented membranes. A highly *b*-oriented but poorly intergrown ETS-4

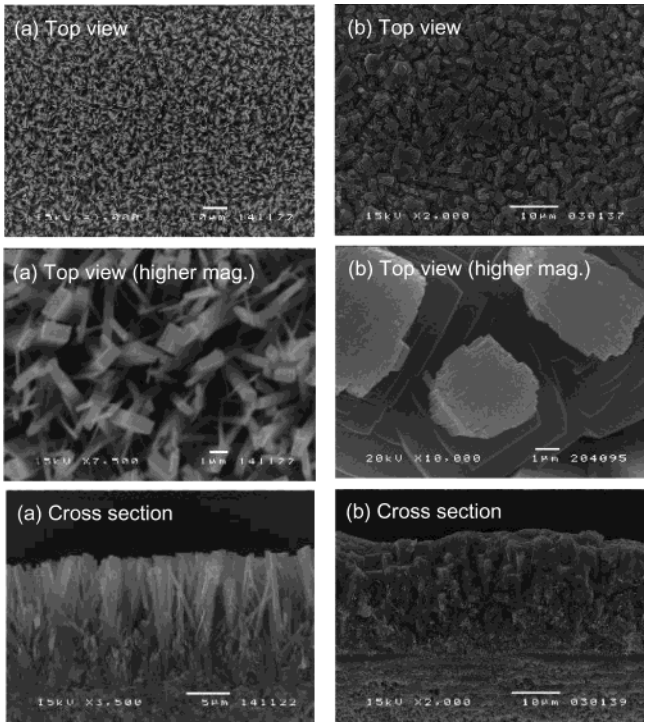

Figure 3. SEM images of the ETS-4 precursor layer (a), and of the ETS-10/-4 film synthesized by heteroepitaxial growth on the ETS-4 precursor layers after 20 h (b).

precursor layer was prepared on an asymmetric porous titania substrate using the secondary growth technique described elsewhere.[18] The nonintergrown needlelike ETS-4 precursor layer was then subjected to secondary growth at 200 °C for various times using a mixture with molar composition of 5.71 SiO_2:1 TiO_2:1.9 KF:7.2 NaOH:168.25 H_2O, which led to the growth of ETS-10. For the synthesis, sodium silicate solution (Aldrich, 27% SiO_2, 14% NaOH) and titanium (III) chloride solution (Fisher Scientific, 10%, stabilized with HCl) were used as a Si and a Ti source, respectively.

Figure 3 shows initial and final images of the ETS-10/-4 film (the time-evolution of the film is provided as Supporting Information). ETS-10 starts growing on the ETS-4 crystals of the precursor layer, eventually filling the gaps between the ETS-4 crystals. That leads to a well-intergrown ETS-10/-4 membrane. From the epitaxial relationship as described above (see Figures 1 and 2) and the preferred orientation of the ETS-4 layer, it is expected that the ETS-10 crystals will be *a* (or, equivalently, *b)*-out-of-plane oriented. This is corroborated by the SEM top view images of the film (compare Figures 3b and 2d) and by analysis of X-ray diffraction (XRD) results. In previous reports, analysis of the preferred orientation of molecular sieve films has been performed by pole figure analysis,[9,10] grazing incidence X-ray diffraction,[28] and at the qualitative level by use of XRD data collected in a Bragg−Brentano geometry.[9,29] For the preliminary account of this communication, the analysis follows the latter approach. Figure 4 shows XRD patterns collected for ETS-4 (trace A) and ETS-10 (B) powders and from the ETS-4 precursor layer (C) of Figure 3a, and the final ETS-10/-4 film (D) of Figure 3b. XRD patterns at various stages of growth are provided as Supporting Information. A comparison of trace A and C of Figure 4 confirms the *b*-out-of-plane orientation of the ETS-4 precursor layer.[18] Trace D, along with the reflections corresponding to the oriented ETS-4 film, clearly shows the appearance of ETS-10 peaks however, with drastic changes in the relative intensities compared to the powder pattern of trace (B). An unambiguous evidence of *a* (or *b)*-out-of-plane preferred orientation is provided by comparison

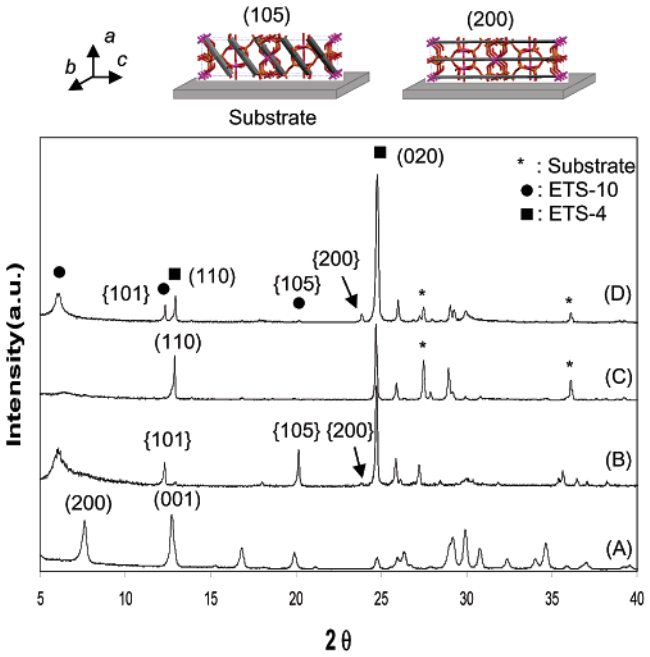

Figure 4. X-ray diffraction patterns. (A) ETS-4 powder, (B) ETS-10 powder, (C) ETS-4 precursor layer, and (D) ETS-10/-4 film grown for 20 h. Indexing of ETS-10 is based on the superposition model by Wang et al.[30] The schemes show the orientation of the (105) and (200) planes with respect to the substrate for *a*-out-of-plane oriented ETS-10.

of the {105} and {200} reflections. The crystallographic preferred orientation, CPO, for these reflections is larger than 50, indicating strong orientation.[31]

The extension of the secondary growth procedure to include heteroepitaxial growth as described here should be applicable in other microporous molecular sieves. For example, zeolite beta (BEA) is known to grow by a similar epitaxial relation on SSZ-31 needles.[26] On the basis of the method presented here, *b*-/*a*-out-of-plane-oriented zeolite beta films could be grown on *c*-oriented films of SSZ-31. More interestingly, the orientation of molecular sieve membranes fabricated by heteroepitaxial growth can be adjusted by changing the orientation of the precursor layers. For example, a *c*-oriented ETS-10 membrane could be fabricated on an *a*-oriented ETS-4 precursor layer.

Acknowledgment. We acknowledge support from the NSF, DOE, NASA (Microgravity) and Engelhard Co.

Supporting Information Available: Images of heteroepitaxially grown ETS-10 crystals on ETS-4 powder and large single crystals (10 μm × 100 μm × 10 μm); time-evolution of the ETS-10/-4 membrane along with XRD patterns (PDF). This material is available free of charge via the Internet at http://pubs.acs.org.

References

(1) Bein, T. *Chem. Mater.* **1996**, *8*, 1636−1653.
(2) Davis, M. E. *Nature* **2002**, *417*, 813−821.
(3) Tsapatsis, M.; Xomeritakis, G.; Hillhouse, H.; Nair, S.; Nikolakis, V.; Bonilla, G.; Lai, Z. *Cattech* **2000**, *3*, 148−158.
(4) Caro, J.; Noack, M.; Kolsch, P.; Schafer, R. *Micropor. Mesopor. Mater.* **2000**, *38*, 3−24.
(5) Ozin, G. A.; Kuperman, A.; Stein, A. *Angew. Chem., Int. Ed. Engl.* **1989**, *28*, 359−376.
(6) Funke, H. H.; Kovalchick, M. G.; Falconer, J. L.; Noble, D. *Ind. Eng. Chem. Res.* **1996**, *35*, 1575−1582.
(7) Wang, Z. B.; Yan, Y. S. *Chem. Mater.* **2001**, *13*, 1101−1107.
(8) Choi, S. Y.; Lee, Y. J.; Park, Y. S.; Ha, K.; Yoon, K. B. *J. Am. Chem. Soc.* **2000**, *122*, 5201−5209.
(9) Boudreau, L. C.; Tsapatsis, M. *Chem. Mater.* **1997**, *9*, 1705−1709.
(10) Gouzinis, A.; Tsapatsis, M. *Chem. Mater.* **1998**, *10*, 2497−2504.
(11) Lovallo, M. C.; Tsapatsis, M. *AIChE J.* **1996**, *42*, 3020−3029.
(12) Xomeritakis, G.; Lai, Z.; Tsapatsis, M. *Ind. Eng. Chem. Res.* **2001**, *40*, 544−552.
(13) Jansen, J. C.; Rosmalen, G. M. *J. Cryst. Growth* **1993**, *128*, 1150−1156.
(14) Balkus, K. J.; Munoz, T.; Gimon-Kinsel, M. E. *Chem. Mater.* **1998**, *10*, 464−466.
(15) Mintova, S.; Hedlund, J.; Schoeman, B.; Valtchev, V.; Sterte, J. *Chem. Commun.* **1997**, *1*, 15−16.
(16) Hedlund, J.; Sterte, J.; Anthonis, M.; Bons, A. J.; Carstensen, B.; Corcoran, N.; Cox, D.; Deckman, H.; De Gijnst, W.; de Moor, P. P.; Lai, F.; McHenry, J.; Mortier, W.; Reinso, J. *Micro. Meso. Mater.* **2002**, *52*, 179−189.
(17) Kondo, M.; Komori, M.; Kita, H.; Okamoto, K. *J. Membr. Sci.* **1997**, *133*, 133−141.
(18) Braunbarth, C. M.; Boudreau, L.; Tsapatsis, M. *J. Membr. Sci.* **2000**, *174*, 31.
(19) Anderson, M. W.; Terasaki, O.; Ohsuna, T.; Malley, P. J. O.; Philippou, A.; MacKay, S. P.; Ferreira, A.; Rocha, J.; Lidin, S. *Philos. Mag. B* **1995**, *71*, 813−841.
(20) Nair, S.; Jeong, H.-K.; Chandrasekaran, A.; Braunbarth, C. M.; Tsapatsis, M.; Kuznicki, S. M. *Chem. Mater.* **2001**, *13*, 4247−4254.
(21) Braunbarth, C.; Hillhouse, H. W.; Nair, S.; Tsapatsis, M.; Burton, A.; Lobo, R. F.; Jabubinas, R. M.; Kuznicki, S. M. *Chem. Mater.* **2000**, *12*, 1857−1865.
(22) Kuznicki, S. M.; Bell, V. A.; Nair, S.; Hillhouse, H. W.; Jacubina, R. M.; Braunbarth, C. M., Toby, B. H.; Tsapatsis, M. *Nature* **2001**, *412*, 720−724.
(23) Borello, E.; Lamberti, C.; Bordiga, S.; Zecchina A.; Arean, C. O. *Appl. Phys. Lett.* **1997**, *71*, 2319−2321.
(24) Okubo, T.; Wakihara, T.; Plevert, J.; Nair, S.; Tsapatsis, M.; Ogawa, Y.; Komiyama, H.; Yoshimura, M.; Davis, M. E. *Angew. Chem., Int. Ed.* **2001**, *40*, 1069−1071.
(25) Porcher, F.; Dusausoy, Y.; Souhassou, M.; Lecomte, C. *Miner. Magn.* **2000**, *64*, 1−8.
(26) Nair, S.; Villaescusa. L. A.; Camblor, M. A.; Tsapatsis, M. *Chem. Commun.* **1999**, 911−922.
(27) Goossens, A. M.; Wouters, B. H.; Buschmann, V.; Martens, J. A. *Adv. Mater.* **1999**, *11*, 561−564.
(28) Metzger, T. H.; Mintova, S.; Bein, T. *Micropor. Mesopor. Mater.* **2001**, *43*, 191−200.
(29) Verduijn, J. P.; Bons, A.-J.; Anthonis, M. H. C.; Czarnetzki, L. R. WO 96/01683, 1996.
(30) Wang, X.; Jacobson, A. J. *Chem. Commun.* **1999**, 973−974.
(31) The CPO for trace B and D is calculated[29] using

$$\mathrm{CPO}_{200/105} = \left[\left(\frac{I_{200}}{I_{105}}\right)_{\mathrm{D}} - \left(\frac{I_{200}}{I_{105}}\right)_{\mathrm{B}}\right] \Big/ \left(\frac{I_{200}}{I_{105}}\right)_{\mathrm{B}}$$

where I is the integrated intensity of the corresponding reflection at the indicated trace.

JA020947W